

Review Article

Beyond X-rays: an overview of emerging structural biology methods

Jason E. Schaffer, Vandna Kukshal, Justin J. Miller, Vivian Kitainda and  Joseph M. Jez

Department of Biology, One Brookings Drive, Campus Box 1137, Washington University in St. Louis, St. Louis, MO 63130, U.S.A.

Correspondence: Joseph M. Jez (jjez@wustl.edu)

Structural biologists rely on X-ray crystallography as the main technique for determining the three-dimensional structures of macromolecules; however, in recent years, new methods that go beyond X-ray-based technologies are broadening the selection of tools to understand molecular structure and function. Simultaneously, national facilities are developing programming tools and maintaining personnel to aid novice structural biologists in *de novo* structure determination. The combination of X-ray free electron lasers (XFELs) and serial femtosecond crystallography (SFX) now enable time-resolved structure determination that allows for capture of dynamic processes, such as reaction mechanism and conformational flexibility. XFEL and SFX, along with microcrystal electron diffraction (MicroED), help side-step the need for large crystals for structural studies. Moreover, advances in cryogenic electron microscopy (cryo-EM) as a tool for structure determination is revolutionizing how difficult to crystallize macromolecules and/or complexes can be visualized at the atomic scale. This review aims to provide a broad overview of these new methods and to guide readers to more in-depth literature of these methods.

Introduction

Over the last 70 years, the approaches and techniques used for scientific inquiry have rapidly progressed. This is no different for the field of structural biology. While the first structural elucidation of a small molecule crystal took place over 100 years ago, the structural study of large biomolecules came into its own during the mid-20th Century with the elucidation of the crystal structures of myoglobin and hemoglobin by Kendrew and Perutz [1,2]. In principle, crystalline macromolecules are exposed to an X-ray beam. Each atom in the crystalline sample diffracts the X-ray, resulting in a discrete diffraction pattern and a molecular two-dimensional view of the crystal lattice. Subsequently, the crystal may be rotated within the beam, and multiple images collected to reconstruct a three-dimensional model of the macromolecule. Since the first macromolecular structures, technological advances in instrumentation, computing, automation, and data collection have pushed the field forward at a remarkable pace. The first X-ray crystal structures of proteins took decades to solve as the tools, methods, and technology for structure determination and visualization were developed. Now, the same process from diffraction to three-dimensional structure can take minutes. These advances open structural biology to scientists in all disciplines.

The source of X-rays used by Kendrew and Perutz for their structural characterization of myoglobin and hemoglobin were X-ray vacuum tubes. While vacuum tubes were cutting edge in the 1950's, they required significant effort to maintain [3]. Now, synchrotron radiation sources are readily available at national laboratories (i.e. user facilities). These synchrotron sources produce better beam characteristics and are brighter than vacuum tubes, enabling rapid and high-resolution structural determination. Importantly, these user facilities are staffed with experts who aid both novice and expert structural biologists with protein crystallography experiments. Planned upgrades at various synchrotron facilities will increase beam performance by several orders of magnitude within the coming decade [4]. Simultaneously, alternative light sources, such as X-ray free electron lasers (XFEL), are in

Received: 29 November 2020

Revised: 27 December 2020

Accepted: 20 January 2021

Version of Record published:

4 February 2021

development and have the potential to increase the brightness of beams by nine orders of magnitude, while simultaneously achieving pulse lengths on the order of femtoseconds. These two feats enable serial data collection and time-resolved diffraction experiments [5]. A more in-depth look at the capabilities and current achievements of XFEL is included in this review.

Complementing advancements in X-ray sources, detection methods, and computational power have dramatically improved. Early X-ray diffraction experiments recorded data on photographic films that were then converted into physical models constructed by researchers. Modern detectors, often hybrid photon counting detectors, allow for millisecond detection times of diffracted energy across a wide dynamic range [6]. Rapid detection and initial processing of diffraction data also enables quick determination of the quality data feasibility of a given sample. With modern robotic setups, samples can rapidly be moved from cryogenic storage to the beam path and screened for diffraction. The same robotic apparatus is capable of then rotating samples for extended data collection. This allows for the screening of multiple samples for collection of a complete data set in less than ten minutes. In parallel, modern computer modeling software bypasses the laborious construction of physical models from raw data and can often automatically build the initial three-dimensional model [3]. Data processing and structure determination software is often provided by the user facility to accelerate structure determination on-site.

Along with the increased capabilities of structural biology facilities, advancements in techniques such as heterologous protein expression enable production of high sample quantities and at purities previously unavailable [7]. Now, new techniques are eliminating the need for large, pristine crystal samples. Serial crystallography, grid and plate scanning, microcrystal electron diffraction, *in situ* and *in cellulo* detection, and structural determination are all lowering the barrier of sample quality needed to obtain usable data [8,9]. Continued development in this vein promises to further decrease the difficulty in the hardest step of protein crystallography, i.e. obtaining a usable crystal. As will be discussed later, advances in technology like cryogenic electron microscopy (cryo-EM) can side-step the need for protein crystallization, but still require the production of pure protein samples in sufficient quantities for data collection.

In addition to enabling the remarkable scientific achievements of structural biology, access to beamline facilities helps to demystify the process and to grow the user base for these resources [4]. Access to staff who are willing to aide in all steps of the research process from data collection to structure determination has led to unprecedented ease-of-access to X-ray crystallography for researchers across a diverse set of disciplines. Improved accessibility is critical for researchers in the plant and life sciences, medicine, and pharmaceutical industry to obtain three-dimensional structures of their macromolecules of interest. Now, the next structural biology revolution is starting and is already expanding how scientists reveal Nature's machinery. Here we provide an overview of new structural biology approaches that are going beyond traditional X-ray diffraction experiments.

X-ray free electron lasers and serial femtosecond crystallography

Structure determination of proteins at the atomic level is an essential step for understanding protein function, reaction mechanism, and conformational dynamics. Traditional macromolecule X-ray crystallography remains a powerful tool for understanding protein structures, but the method has limitations, including radiation damage (which can impact data quality), the essential need for good quality protein crystals, and typically static image of the resulting protein structure. The advent of X-ray free electron lasers (XFELs) and serial femtosecond crystallography (SFX) helps address some of these limitations.

XFEL sources accelerate electrons to high energies that produce X-rays with the properties of laser light in high-intensity pulses on the femtosecond (10^{-15} s) timescale and at more than a billion-fold brighter intensity than current synchrotron X-ray sources [10]. Currently, five XFEL facilities are operational world-wide, including the Linac Coherent Light Source (LCLS; U.S.A.), SPring-8 Angstrom Compact free electron LAser (SCALA; Japan), European XFEL (Germany), Pohang Accelerator Laboratory-XFEL (PAL-XFEL; South Korea), and SwissFEL (Switzerland) [11]. XFELs enable the rapid delivery of a high-intensity pulse for collection of diffraction data on a crystal before radiation damage occurs — ‘diffraction before destruction.’ [12]. Because the intense radiation of the energy pulse destroys the crystal, the data collection strategy and physical set-up for placing crystals into the beam used for these experiments differs from macromolecular crystallography, in which a single crystal is rotated within the X-ray beam to collect a complete diffraction dataset. With an XFEL energy source, data collection requires the use of SFX. In this approach, multiple single-crystal diffraction

images (one from each crystal before its destruction) are collected, then combined for a full set of data for final structure determination. For example, in one of the first demonstrations of this technology, more than 3 million diffraction patterns, each from a single nanocrystal of a cyanobacterial Photosystem I, were used to solve the structure and to validate this technology [13].

SFX data collection requires the constant delivery of crystals into the beam with each crystal contributing to the total data set (Figure 1A). This process requires large quantities of microcrystals (100 nm to 10 μm) grown using a variety of methods, such as inducing nucleation in traditional vapor diffusion methods, mechanically crushed large crystals, and lipidic cubic phase crystallization for membrane proteins [14–16]. While traditional macromolecular crystallography delivers crystals on a single cryoloop, in XFELs millions of individual microcrystals are delivered using either liquid jet injection devices or solid supports, like fixed-target wafers and chips [17,18]. The coordinated delivery of one crystal for one XFEL pulse, on the timescale of <50 femtoseconds, also required the development of new data collection hardware. To accommodate the rapid rate of data collection, a novel charge-coupled device detector with the capability to integrate high photon counts and fast readout speeds that match the high repetition rate of pulses are essential [19–21]. Due to sample delivery and shot-to-shot variation of crystal quality and beam characteristics, the data obtained through the combination of XFELs and SFX contains substantial variation. As a result, pre-processing of the diffraction data is an essential step to clean-up frames, correct for background changes, and to identify useful Bragg reflections from thousands of frames. This is achieved by using specialized software packages, such as Cheetah [22]. After pre-processing, data indexing and integration employs algorithms shared with traditional macromolecular crystallography [23].

Since the first proof-of-principle structure of Photosystem I [13], SFX has progressed on all fronts, from the advancement of crystal delivery systems to improved data collection and evaluation procedures. Nearly 372 structures (366 proteins and 6 RNAs) have been deposited to Protein Data Bank solved using SFX with more than 75% of structures solved at 1.5–3.5 \AA resolution. Most of the protein structures determined by SFX have been phased by the molecular replacement method, which requires a homologous template structure to solve the phase problem; however, recently de novo phasing techniques have also been implemented successfully for XFEL [24–26]. The combination of XFEL and SFX can achieve high-resolution structure determination, but the XFEL timescale enables crystallographers to examine rapid structural dynamics that are time-dependent and radiation-sensitive.

Time-resolved SFX using XFELs opens the field to dynamical studies in the femtosecond to millisecond timescale by using photoactivation or chemical mixing-initiated enzymatic reactions [27]. The reaction cycle of a protein of interest can be triggered and followed by time-resolved capture of diffraction images (Figure 1B). For example, each microcrystal is ‘triggered’ to start a reaction, then travels for a defined time before entering

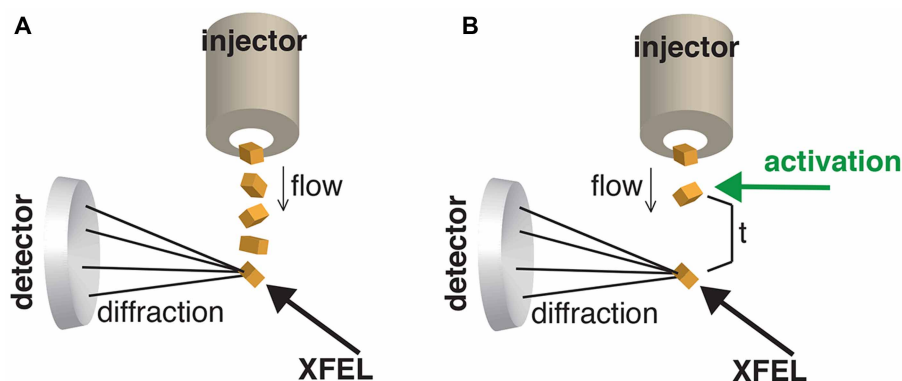


Figure 1. Overview of X-ray free electron laser (XFELs) and serial femtosecond crystallography (SFX) experimental set-up.

(A) Basic XFEL-SFX set-up. Crystals are individually injected along a flow-path into the XFEL. As each pulse hits the crystal, diffraction data is collected so that each randomly oriented crystal provides one diffraction image before its destruction. (B) Time-resolved SFX using XFEL. Injection of each crystal into the flow occurs with a defined timing (t) between activation of the crystal and the XFEL pulse. This set-up allows the protein to perform its function for a set time before data is collected.

the XFEL and the data collection energy pulse. In subsequent experiments, changing the time before the data collection pulse and/or using other triggers can lead to a series of structural stop-motion images of protein as it performs its function.

Photosynthetic reaction centers are ideal test cases for this technology. For example, time-resolved experiments using the cyanobacterial photosystem II combined femtosecond X-ray spectroscopy to step the complex through different stages in its reaction cycle to provide snapshots of the water oxidation cycle as it progressed from dark to light excited states [28,29]. Recent work clarified the mechanism of photosystem II using time-resolved SFX [30]. The rapid technical and experimental development in SFX and its application to understand real-time protein structures opens a path to solve hard to crystallize protein structures and to uncover the dynamics of various reaction mechanisms.

The use of serial data collection is also inspiring efforts to establish serial macromolecular crystallography at synchrotron X-ray beamlines by combining new sample delivery methods, high-intensity X-ray microbeams comparable to the size of microcrystals, and rapid-read detectors [31]. The data collection, processing, and structure determination in serial macromolecular crystallography are similar to that of SFX and relies on a 'one crystal - one shot' approach. Unlike SFX, due to exposure to high-intensity X-rays at room temperature, the radiation damage cannot be ignored and may be led to structure factor ambiguity; however, nearly 100 structures determined by serial macromolecular crystallography are available in PDB with resolution reaching up to 1.5 Å. Moreover, time-resolved experiments in the millisecond range were also made possible by using a microfluidic injector and setting a time delay between the reaction activation and X-ray intersection point opened the way for dynamic studies at synchrotron radiation [32]. Once again photoactive proteins from plants are a rich source of material for these experiments with dark and light-excited state structures of phototropin-2 and the UVR8 ultraviolet light photoreceptor recently determined using serial crystallography methods [33,34]. The ability to capture structural dynamics of proteins in actions using either XFEL and SFX or serial crystallography promise to play an ever-increasing role in plant structural biology in the coming years.

Microcrystal electron diffraction

Although X-ray crystallography experiments are irreplaceable, some proteins stubbornly refuse to form crystals large and homogenous enough for traditional X-ray crystallography. Microcrystal electron diffraction (MicroED), by contrast, excels with crystals on the order of 0.5–1 µm thick. The workflow for MicroED blends elements of X-ray crystallography and cryo-EM [35,36]. Microcrystals are loaded onto a transmission electron microscopy grid and frozen as in cryo-EM. Once placed in the electron microscope, individual crystals are exposed to the electron beam, and the resulting diffraction patterns are captured (Figure 2). As with X-ray crystallography, the sample is then tilted to allow for the capture of additional viewing angles for acquisition of a complete dataset.

Due to the similarity between MicroED and X-ray crystallography datasets, many of the same programs developed for X-ray crystallography also function for MicroED. These programs vary in levels of user-friendliness for novice crystallographers but do allow for new users to learn crystallography and solve crystal structures; however, several important differences do exist between the two techniques. Because the wavelengths of electron beams are significantly shorter than for X-rays, only partial diffraction patterns are collected on a single image for MicroED. This results in initial indexing being more difficult to correctly perform with MicroED datasets than with X-ray datasets and requires multiple images tilted at least 20° apart from one another for complete indexing [37]. MicroED also varies from X-ray crystallography in the determination of novel crystal structures. When molecular replacement fails in X-ray crystallography, users can attempt to use heavy metal phasing, single-wavelength anomalous diffraction (SAD), or multiple-wavelength anomalous diffraction (MAD) to solve the structure. Unfortunately, electron beams do not yield any anomalous signal at the wavelengths used during MicroED, which prevents these techniques from being used. Isomorphous replacement can still be used to solve *de novo* structures.

The ability to analyze small crystals, or mechanically disrupted large crystals is an exceptionally useful aspect of MicroED [38]. One paramount benefit of smaller crystal size is the time required for compounds to diffuse in and out of the crystal lattice. With quick equilibration between the crystal and the surrounding solution, it is feasibly possible to visualize time-resolved movement of binding and reaction events of macromolecules. The time resolution for these studies is likely limited to the rate of sample preparation and vitrification, the latter of which can occur on the microsecond time scale [39].

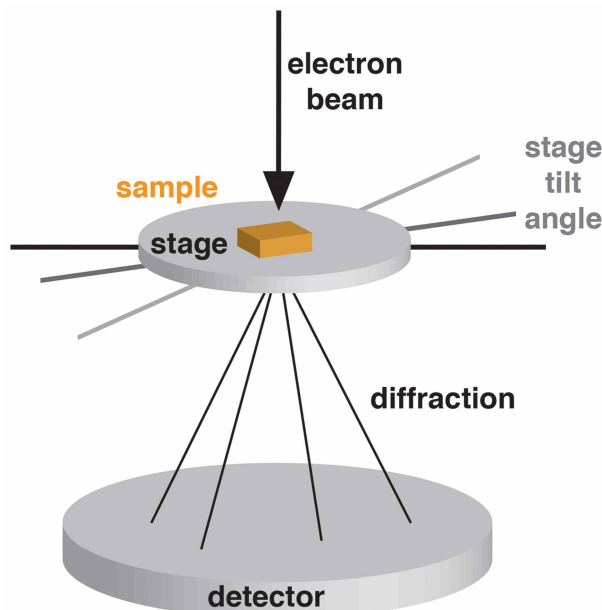


Figure 2. Overview of microcrystal electron diffraction (MicroED) experimental set-up.

Multiple microcrystals are embedded in a sample matrix. Within the electron microscope, the beam is focused on the sample and the stage tilted to generate multiple diffraction images for structure determination.

While only 13 unique protein structures have been solved with MicroED and deposited in the PDB, we anticipate that MicroED will become a popular technique for crystallographers. Indeed, this technique has already proven capable of generating extremely high-resolution structures, most notably a 1.50 Å structure of proteinase K [40]. Furthermore, the popularization and spread of Cryo-EM has led many laboratories to have access to electron microscopes capable of collecting MicroED datasets. This technique has been incredibly useful in the solving of several previously unsolvable crystal structures including, most notably, α -synuclein [41]. MicroED has also resulted in structural solutions for numerous small molecules and peptides. We are excited to see the novel structures and information MicroED will bring to plant biology.

Cryogenic-electron microscopy

Cryo-EM has emerged as one of the mainstream methods in structural biology for determining the architecture of cells, viruses, and protein assemblies in their native state at molecular resolution [42–44]. Cryo-EM encompasses a range of experimental methods, all based upon the principle of imaging radiation-sensitive specimens in a transmission electron microscope under cryogenic conditions. Its main subdisciplines are cryo-electron tomography (cryo-ET) and single-particle cryo-EM, both of which have previously been described in more detail [45–47]. As frozen specimens can tolerate higher electron doses, images collected on the electron microscope are captured at ultra-low temperatures, enabling a higher signal-to-noise ratios. Multiple identical particles are averaged to further increase the signal-to-noise ratio of cryo-EM. These two concepts form the basis of modern high-resolution biological electron microscopy [45].

Cryo-ET fills in a critical gap in cell biology - visualizing one-of-a-kind, structurally heterogeneous entities at resolutions between 50 and 100 Å, which is significantly better than can be achieved using optical microscopy [45]. For example, cells either grown on or deposited upon electron microscopy grid in a layer up to 10 μm thick for plunge freezing. Similarly, tissues up to 200 μm thick can be prepared using a high-pressure freezer. As specimens need to be <0.5 microns for sample penetrance of the electron beam, thicker samples require sectioning before imaging, which can be carried out using focused ion-beam milling for cells or a cryo-microtome for tissues. This method is time consuming and the throughput of sample preparation by this method is currently limited, as ~5 sample sections can be produced on a machine per day [48]. Future improvements could potentially increase the efficiency of this method.

For cryo-ET data collection, a series of images are collected for each section with each image taken at a different tilt relative to the incident electron beam [49]. This is a process similar to MicroED, except that crystals are not used as samples and diffraction data not collected. A blurring effect on the images can be caused by the beam-induced motion of the specimen, but new cameras and software (based on direct electron detection) are able to correct this, enabling higher resolution analysis. The images are combined computationally to generate tomograms, which are three-dimensional images of the specimen. In addition to averaging tomograms, the Volta phase plate technique, which increases the contrast of images, can also be used to achieve better resolutions [48]. Depending on the protein being examined, subcomponents whose structures have been previously determined by either X-ray crystallography or NMR analyses can be fitted reliably into the tomographic density maps to obtain three-dimensional structures at better than ~ 8 Å resolution [45,48]. Recent examples that highlight the versatility and potential of cryo-ET include the imaging of the intact SARS-CoV-2 virus, which was applied to the electron microscopy grid [50], visualization of the lipopolysaccharide-bound surface layer of a bacterial cell using intact cells applied to electron microscopy grid [51], and the use of *Chlamydomonas* cells grown on electron microscopy grids (followed by focused ion-beam milling) for cryo-ET visualization of thylakoid membranes in chloroplasts of the algae [52].

Due to the heterogeneity of cellular structures, cryo-ET data interpretation can be challenging. One way to assign a structure to a protein is to use difference maps between the wild-type and mutant density maps, which show the target as absent densities. Additionally, proteins can be modified with genetically encoded markers, such as SNAP and APEX (enhanced ascorbate peroxidase) tags [53,54], which provide distinctive electron densities that can aid in identifying components of the assembly [48]. Another method for cryo-ET data interpretation is to correlate light microscopic images with cryo-EM structures using fluorescently-labeled molecules. For a successful application of this technique, the area of cryo-compatible super-resolution microscopes and fluorescent dyes needs further development [48]. Eventually, it might be possible to identify a protein from the cryo-ET structure itself, namely 'visual proteomics' [48].

Single-particle cryo-EM is rapidly becoming a powerful structural biology tool to analyze macromolecules and complexes that are difficult to crystallize. The general approach used in cryo-EM can be divided into screening and structure determination steps (Figure 3). For screening, purified protein is typically deposited on a carbon film backed with a support structure for negative staining. Individual particles are selected by hand/automated algorithms on acquired two-dimensional projection images, ideally featuring copies of a complex in different orientations, while statistical methods are used to sort images based on variations in structural features [47]. The goal is to have satisfactory two-dimensional class averages with mono-disperse particles lacking in aggregation and limited heterogeneity before moving to high-resolution data collection and structure determination. Although negative staining is currently used for screening of sample quality, this approach has drawbacks, such as the protein being affected by harsh staining conditions or heavy metal deposition leading to sample aggregation. Moreover, given that sample preparation for high-resolution data collection, described below, uses different conditions and techniques, groups are working to use low-resolution cryo-EM screening to simplify the screening process.

For the next step, sample preparation for high-resolution data collection involves freezing the sample at cryogenic temperatures (vitrification) [47]. During data collection, related images of individual particles are averaged to obtain two-dimensional projection views of the macromolecule, which are used for three-dimensional reconstruction through mathematical techniques. Initial three-dimensional maps provide a starting point for refinement, evaluation, and validation of a cryo-EM structure. Available atomic coordinates of the protein components solved from X-ray or NMR analyses can be fitted into the final structure [45–47]. With current instrumentation and image processing algorithms in single particle cryo-EM analysis, high-resolution three-dimensional maps in the 2–4 Å resolution range can be achieved on a regular basis. As with any method for three-dimensional structure determination, sample preparation and purity are critical [55]. However, these resolutions are not always possible due to the lack of reproducibility of cryo-EM specimens resulting from lack of control over the thickness of the ice layer and the timing of vitrification during sample preparation [48]. Nevertheless, continued improvements in freeze-plunging devices aim to improve the consistency of specimens.

A major drawback to the applicability of cryo-EM in various research areas is how slow and expensive of a process it is. In single-particle cryo-EM, the procedure for initial sample quality evaluation (sample screening) is labor intensive and is performed exclusively on electron microscopes. In the future, some aspects of this procedure could be automated using artificial intelligence technology and evaluated by infrared/UV absorption light microscopy. Similar to the sample screening process, setting up a data acquisition session is a manual

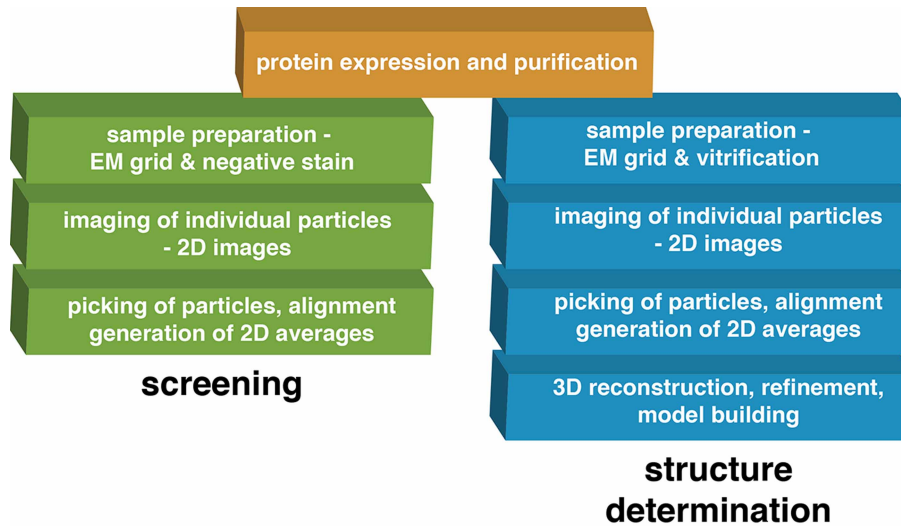


Figure 3. Overview of cryogenic-electron microscopy (cryo-EM) workflow.

Protein expression and purification is the starting point. Initial screening (left, green) to assess sample quality and suitability for further analysis involves preparing the sample for cryo-EM, imaging of individual particles (i.e. collection of two-dimensional images), and generation of two-dimensional class averages. If the sample shows a lack of aggregation and limited heterogeneity, then high-resolution data collection and structure determination can begin (right, blue). The initial steps are similar to the screening process, but the final step of using the two-dimensional averages to construct a three-dimensional map for subsequent refinement and model building begins.

process that takes one to several hours, and thus could also benefit from AI automation in the future [48]. Additionally, the most unproductive step during data acquisition is the wait for the sample stage mechanical drift to settle after a stage move. The acquisition area can be moved optically instead of mechanically, which increases the data acquisition speed from ~1000 to ~5000 images per day [56]. With the more widespread application of this method, there could be a two-fold increase in cryo-EM throughput in the next couple of years. Currently, cryo-EM requires significant human interaction and judgement during data processing and evaluation. The development of automated, robust, and unambiguous data processing pipelines will facilitate the widespread availability and efficiency of cryo-EM. As automated processes develop, the implementation of a real-time metric of data quality and prediction of the achievable resolution from a given number of particles/images will allow researchers to better plan and optimize their microscope sessions [48].

Overall, cryo-EM has made great progress in the past few years and continues to evolve to become a more efficient and routine technique that has potential to be universally adopted among researchers. In plant biology, cryo-EM has provided powerful insights into numerous fundamental plant cellular processes, as recently summarized [57]. To date, more than 30 plant-related macromolecular cryo-EM structures have been determined, such as the plant mitochondrial complex I [58], RNA-rich mitochondrial ribosome [59], mechano-sensitive channel [60], photosystem II light harvesting complex [61], and cytochrome b6f complex [62], and most of these structures solved within the last 3 years. Thus, as cryo-EM becomes a more accessible technique, it promises to enable further discoveries in plant biology within the near future.

Conclusion

Across the field of plant biology, new technologies are accelerating research progress, changing the questions asked, and deepening our understanding of how plants function. Twenty years ago, a plant biochemist would turn to X-ray crystallography. Today, XFELs and SFX, MicroED, and cryo-EM are added to the selection of powerful tools to reveal the workings of Nature's machinery. This review is intended to be a broad overview of these new methods and to serve as a starting point that guides readers to more in-depth treatments of these emerging methods and their amazing capabilities. It will be interesting to see where the application of these tools takes plant biology (and other fields) over the next 20 years.

Summary

- New structural biology methods offer more choice for how to solve the three-dimensional structures of macromolecules.
- X-ray free electron lasers (XFELs) and serial femtosecond crystallography (SFX) enable time-resolved structure determination.
- Microcrystal electron diffraction (MicroED) and cryogenic electron microscopy (cryo-EM) help reduce or eliminate, respectively, the need for large protein crystals for structure determination.
- These emerging technologies are revolutionizing structural biology and opening these tools for a broader range of scientists.

Competing Interests

The authors declare that there are no competing interests associated with the manuscript.

Funding

This work was supported by the National Science Foundation (MCB-1614539 and MCB-1818040).

Author Contribution

All authors contributed to the writing and editing of the manuscript.

Abbreviations

cryo-EM, cryogenic electron microscopy; MicroED, microcrystal electron diffraction; SFX, serial femtosecond crystallography; XFEL, X-ray free electron lasers.

References

- 1 Kendrew, J.C., Bodo, G., Dintzis, H.M., Parrish, R.G., Wyckoff, H. and Phillips, D.C. (1958) A three-dimensional model of the myoglobin molecular obtained by x-ray analysis. *Nature* **181**, 662–666 <https://doi.org/10.1038/181662a0>
- 2 Perutz, M.F., Rossmann, M.G., Cullis, A.F., Muirhead, H., Will, G. and North, A.C.T. (1960) Structure of haemoglobin: a three-dimensional Fourier synthesis at 5.5-Å resolution, obtained by x-ray analysis. *Nature* **185**, 416–422 <https://doi.org/10.1038/185416a0>
- 3 Dauter, Z. and Wlodawer, A. (2016) Progress in protein crystallography. *Protein Pept. Lett.* **23**, 201–210 <https://doi.org/10.2174/0929866523666160106153524>
- 4 Mitchell, E., Kuhn, P. and Garman, E. (1999) Demystifying the synchrotron trip: a first-time user's guide. *Structure* **7**, R111–R121 [https://doi.org/10.1016/S0969-2126\(99\)80063-X](https://doi.org/10.1016/S0969-2126(99)80063-X)
- 5 McNeil, B.W.J. and Thompson, N.R. (2010) X-ray free-electron lasers. *Nat. Photonics* **4**, 814–821 <https://doi.org/10.1038/nphoton.2010.239>
- 6 Förster, A., Brandstetter, S. and Schulze-Briese, C. (2019) Transforming x-ray detection with hybrid photon counting detectors. *Philos. Trans. R. Soc. A* **377**, 20180241 <https://doi.org/10.1098/rsta.2018.0241>
- 7 Rosano, G.L., Morales, E.S. and Ceccarelli, E.A. (2019) New tools for recombinant protein production in *Escherichia coli*: a 5-year update. *Protein Sci.* **28**, 1412–1422 <https://doi.org/10.1002/pro.3668>
- 8 Cheng, R., Huang, C., Hennig, M., Nar, H. and Schnapp, G. (2020) *In situ* crystallography as an emerging method for structure solution of membrane proteins: the case of CCR2A. *FEBS J.* **287**, 866–873 <https://doi.org/10.1111/febs.15098>
- 9 Nass, K., Redecke, L., Perbandt, M., Yefanov, O., Klinge, M., Koopmann, R. et al. (2020) *In cellulo* crystallization of *Trypanosoma brucei* IMP dehydrogenase enables the identification of genuine co-factors. *Nat. Commun.* **11**, 620 <https://doi.org/10.1038/s41467-020-14484-w>
- 10 Bogan, M.J. (2013) X-ray free electron lasers motivate bioanalytical characterization of protein nanocrystals: serial femtosecond crystallography. *Anal. Chem.* **85**, 3464–3461 <https://doi.org/10.1021/ac303716r>
- 11 Emma, P., Akre, R., Arthur, J., Bionta, R., Bostedt, C., Bozek, J. et al. (2010) First lasing and operation of an ångstrom-wavelength free-electron laser. *Nat. Photon.* **4**, 641–647 <https://doi.org/10.1038/nphoton.2010.176>
- 12 Doerr, A. (2011) Diffraction before destruction. *Nat. Methods* **8**, 283 <https://doi.org/10.1038/nmeth0411-283>
- 13 Chapman, H.N., Fromme, P., Barty, A., White, T.A., Kirian, R.A., Aquila, A. et al. (2011) Femtosecond x-ray protein nanocrystallography. *Nature* **470**, 73–77 <https://doi.org/10.1038/nature09750>

14 Kupitz, C., Grotjohann, I., Conrad, C.E., Roy-Chowdhury, S., Fromme, R. and Fromme, P. (2014) Microcrystallization techniques for serial femtosecond crystallography using photosystem II from *Thermosynechococcus elongatus* as a model system. *Philos. Trans. R. Soc. Lond. B Biol. Sci.* **369**, 20130316 <https://doi.org/10.1098/rstb.2013.0316>

15 Redecke, L., Nass, K., DePonte, D.P., White, T.A., Rehders, D., Barty, A. et al. (2013) Natively inhibited *Trypanosoma brucei* cathepsin B structure determined by using an X-ray laser. *Science* **339**, 227–230 <https://doi.org/10.1126/science.1229663>

16 Liu, W., Wacker, D., Wang, C., Abola, E. and Cherezov, V. (2014) Femtosecond crystallography of membrane proteins in the lipidic cubic phase. *Philos. Trans. R. Soc. Lond. B Biol. Sci.* **369**, 20130314 <https://doi.org/10.1098/rstb.2013.0314>

17 Zhao, F.Z., Zhang, B., Yan, E.K., Sun, B., Wang, Z.J., He, J.H. et al. (2019) A guide to sample delivery systems for serial crystallography. *FEBS J.* **286**, 4402–4417 <https://doi.org/10.1111/febs.15099>

18 Hunter, M.S., Seigelke, B., Messerschmidt, M., Williams, G.J., Zatsepin, N.A., Barty, A. et al. (2014) Fixed-target protein serial microcrystallography with an x-ray free electron laser. *Sci. Rep.* **4**, 6026 <https://doi.org/10.1038/srep06026>

19 Johansson, L.C., Stauch, B., Ishchenko, A. and Cherezov, V. (2017) A bright future for serial femtosecond crystallography with XFELs. *Trends Biochem. Sci.* **42**, 749–762 <https://doi.org/10.1016/j.tibs.2017.06.007>

20 Spence, J.C.H. (2017) XFELs for structure and dynamics in biology. *IUCrJ* **4**, 322–339 <https://doi.org/10.1107/S2052252517005760>

21 Martin-Garcia, J.M., Conrad, C.E., Coe, J., Roy-Chowdhury, S. and Fromme, P. (2016) Serial femtosecond crystallography: A revolution in structural biology. *Arch. Biochem. Biophys.* **602**, 32–47 <https://doi.org/10.1016/j.abb.2016.03.036>

22 Barty, A., Kirian, R., Maia, F.R., Hantke, M., Yoon, C.H., White, T.A. et al. (2014) Cheetah: software for high-throughput reduction and analysis of serial femtosecond X-ray diffraction data. *J. Appl. Crystallogr.* **47**, 1118–1131 <https://doi.org/10.1107/S1600576714007626>

23 White, T.A., Mariani, V., Brehm, W., Yefanov, O., Barty, A., Beyerlein, K.R. et al. (2016) Recent developments in CrystFEL. *J. Appl. Crystallogr.* **49**, 680–689 <https://doi.org/10.1107/S1600576716004751>

24 Barends, T.R., Foucar, L., Botha, S., Doak, R.B., Shoeman, R.L., Nass, K. et al. (2014) De novo protein crystal structure determination from X-ray free-electron laser data. *Nature* **505**, 244–247 <https://doi.org/10.1038/nature12773>

25 Nass, K., Meinhart, A., Barends, T.R., Foucar, L., Gorel, A., Aquila, A. et al. (2016) Protein structure determination by single-wavelength anomalous diffraction phasing of X-ray free-electron laser data. *IUCrJ* **3**, 180–191 <https://doi.org/10.1107/S2052252516002980>

26 Nakane, T., Hanashima, S., Suzuki, M., Saiki, H., Hayashi, T., Kakinouchi, K. et al. (2016) Membrane protein structure determination by SAD, SIR, or SIRAS phasing in serial femtosecond crystallography using an iododetergent. *Proc. Natl. Acad. Sci. U.S.A.* **113**, 13039–13044 <https://doi.org/10.1073/pnas.1602531113>

27 Orville, A.M. (2020) Recent results in time-resolved serial femtosecond crystallography at XFELs. *Curr. Opin. Struct. Biol.* **65**, 193–208 <https://doi.org/10.1016/j.sbi.2020.08.011>

28 Kern, J., Alonso-Mori, R., Tran, R., Hattne, J., Gildea, R.J., Echols, N. et al. (2013) Simultaneous femtosecond X-ray spectroscopy and diffraction of photosystem II at room temperature. *Science* **340**, 491–495 <https://doi.org/10.1126/science.1234273>

29 Kupitz, C., Basu, S., Grotjohann, I., Fromme, R., Zatsepin, N.A., Rendek, K.N. et al. (2014) Serial time-resolved crystallography of photosystem II using a femtosecond X-ray laser. *Nature* **513**, 261–265 <https://doi.org/10.1038/nature13453>

30 Suga, M., Akita, F., Yamashita, K., Nakajima, Y., Ueno, G., Li, H. et al. (2019) An oxyl/oxo mechanism for oxygen–oxygen coupling in PSII revealed by an x-ray free-electron laser. *Science* **366**, 334–338 <https://doi.org/10.1126/science.aax6998>

31 Stellato, F., Oberthür, D., Liang, M., Bean, R., Gati, C., Yefanov, O. et al. (2014) Room-temperature macromolecular serial crystallography using synchrotron radiation. *IUCrJ* **1**, 204–212 <https://doi.org/10.1107/S2052252514010070>

32 Weinert, T., Skopintsev, P., James, D., Dworkowski, F., Panepucci, E., Kekilli, D. et al. (2019) Proton uptake mechanisms in bacteriorhodopsin captured by serial synchrotron crystallography. *Science* **365**, 61–65 <https://doi.org/10.1126/science.aaw8634>

33 Ren, Z., Ayhan, M., Bandara, S., Bowatte, K., Kumarapperuma, I., Gunawardana, S. et al. (2018) Crystal-on-crystal chips for *in situ* serial diffraction at room temperature. *Lab. Chip.* **18**, 2246–2256 <https://doi.org/10.1039/C8LC00489G>

34 Aumonier, S., Santoni, G., Gotthard, G., von Stetten, D., Leonard, G.A. and Royant, A. (2020) Millisecond time-resolved serial oscillation crystallography of a blue-light photoreceptor at a synchrotron. *IUCrJ* **7**, 728–736 <https://doi.org/10.1107/S2052252520007411>

35 Gonen, T. (2013) The collection of high-resolution electron diffraction data. *Methods Mol. Biol.* **955**, 153–169 https://doi.org/10.1007/978-1-62703-176-9_9

36 Shi, D., Nannenga, B.L., de la Cruz, M.J., Liu, J., Sawtelle, S., Calero, G. et al. (2016) The collection of MicroED data for macromolecular crystallography. *Nat. Protoc.* **11**, 895–904 <https://doi.org/10.1038/nprot.2016.046>

37 Hattne, J., Reyes, F.E., Nannenga, B.L., Shi, D., de la Cruz, M.J., Leslie, A.G. et al. (2015) MicroED data collection and processing. *Acta Crystallogr. A* **71**, 353–360 <https://doi.org/10.1107/S2053273315010669>

38 de la Cruz, M.J., Hattne, J., Shi, D., Seidler, P., Rodriguez, J., Reyes, F.E. et al. (2017) Atomic-resolution structures from fragmented protein crystals with the cryoEM method MicroED. *Nat. Methods* **14**, 399–402 <https://doi.org/10.1038/nmeth.4178>

39 Nannenga, B.L. and Gonen, T. (2019) The cryo-EM method microcrystal electron diffraction (MicroED). *Nat. Methods* **16**, 369–379 <https://doi.org/10.1038/s41592-019-0395-x>

40 Zhou, H., Luo, Z. and Li, X. (2019) Using focus ion beam to prepare crystal lamella for electron diffraction. *J. Struct. Biol.* **205**, 59–64 <https://doi.org/10.1016/j.jsb.2019.02.004>

41 Rodriguez, J.A., Ivanova, M.I., Sawaya, M.R., Cascio, D., Reyes, F.E., Shi, D. et al. (2015) Structure of the toxic core of α -synuclein from invisible crystals. *Nature* **525**, 486–490 <https://doi.org/10.1038/nature15368>

42 Orlova, E.V. and Saibil, H.R. (2011) Structural analysis of macromolecular assemblies by electron microscopy. *Chem. Rev.* **111**, 7710–7748 <https://doi.org/10.1021/cr100353t>

43 Lau, W.C. and Rubinstein, J.L. (2013) Single particle electron microscopy. *Methods Mol. Biol.* **955**, 401–426 https://doi.org/10.1007/978-1-62703-176-9_22

44 Bai, X.C., McMullan, G. and Scheres, S.H. (2015) How cryo-EM is revolutionizing structural biology. *Trends Biochem. Sci.* **40**, 49–57 <https://doi.org/10.1016/j.tibs.2014.10.005>

45 Milne, J.L., Borgnia, M.J., Bartesaghi, A., Tran, E.E., Earl, L.A., Schauder, D.M. et al. (2013) Cryo-electron microscopy: a primer for the non-microscopist. *FEBS J.* **280**, 28–45 <https://doi.org/10.1111/febs.12078>

46 Cheng, Y., Grigorieff, N., Penczek, P.A. and Walz, T. (2015) A primer to single-particle cryo-electron microscopy. *Cell* **161**, 438–449 <https://doi.org/10.1016/j.cell.2015.03.050>

47 Lyumkis, D. (2019) Challenges and opportunities in cryo-EM single-particle analysis. *J. Biol. Chem.* **294**, 5181–5197 <https://doi.org/10.1074/jbc.REV118.005602>

48 Danev, R., Yanagisawa, H. and Kikkawa, M. (2019) Cryo-electron microscopy methodology: current aspects and future directions. *Trends Biochem. Sci.* **44**, 837–848 <https://doi.org/10.1016/j.tibs.2019.04.008>

49 Chreifi, G., Chen, S., Metskas, L.A., Kaplan, M. and Jensen, G.J. (2019) Rapid tilt-series acquisition for electron cryotomography. *J. Struct. Biol.* **205**, 163–169 <https://doi.org/10.1016/j.jsb.2018.12.008>

50 Yao, H., Song, Y., Chen, Y., Wu, N., Xu, J., Sun, C. et al. (2020) Molecular architecture of the SARS-CoV-2 virus. *Cell* **183**, 730–738 <https://doi.org/10.1016/j.cell.2020.09.018>

51 von Kügelgen, A., Tang, H., Hardy, G.G., Kureisaite-Ciziene, D., Brun, Y.V., Stansfeld, P.J. et al. (2020) In situ structure of an intact lipopolysaccharide-bound bacterial surface layer. *Cell* **180**, 348–358 <https://doi.org/10.1016/j.cell.2019.12.006>

52 Wietrzynski, W., Schaffer, M., Tegunov, D., Albert, S., Kanazawa, A., Plitzko, J.M. et al. (2020) Charting the native architecture of *Chlamydomonas* thylakoid membranes with single-molecule precision. *eLife* **9**, e53740 <https://doi.org/10.7554/eLife.53740>

53 Keppler, A., Gendreizig, S., Gronemeyer, T., Pick, H., Vogel, H. and Johnson, K. (2003) A general method for the covalent labeling of fusion proteins with small molecules *in vivo*. *Nat. Biotechnol.* **21**, 86–89 <https://doi.org/10.1038/nbt765>

54 Martell, J.D., Deerinck, T.J., Sancak, Y., Poulos, T.L., Mootha, V.K., Sosinsky, G.E. et al. (2012) Engineered ascorbate peroxidase as a genetically encoded reporter for electron microscopy. *Nat. Biotechnol.* **30**, 1143–1148 <https://doi.org/10.1038/nbt.2375>

55 Passmore, L.A. and Russo, C.J. (2016) Specimen preparation for high-resolution cryo-EM. *Methods Enzymol.* **579**, 51–86 <https://doi.org/10.1016/bs.mie.2016.04.011>

56 Kim, L.Y., Rice, W.J., Eng, E.T., Kopylov, M., Cheng, A., Raczkowski, A.M. et al. (2018) Benchmarking cryo-EM single particle analysis workflow. *Front. Mol. Biosci.* **5**, 50 <https://doi.org/10.3389/fmolsb.2018.00050>

57 Otegui, M.S. and Pennington, J.G. (2019) Electron tomography in plant cell biology. *Microscopy* **68**, 69–79 <https://doi.org/10.1093/jmicro/dfy133>

58 Soufari, H., Parrot, C., Kuhn, L., Waltz, F. and Hashem, Y. (2020) Specific features and assembly of the plant mitochondrial complex I revealed by cryo-EM. *Nat. Commun.* **11**, 5195 <https://doi.org/10.1038/s41467-020-18814-w>

59 Waltz, F., Soufari, H., Bochler, A., Giegé, P. and Hashem, Y. (2020) Cryo-EM structure of the RNA-rich plant mitochondrial ribosome. *Nat. Plants* **6**, 377–383 <https://doi.org/10.1038/s41477-020-0631-5>

60 Deng, Z., Maksaev, G., Schlegel, A.M., Zhang, J., Rau, M., Fitzpatrick, J.A.J. et al. (2020) Structural mechanism for gating of a eukaryotic mechanosensitive channel of small conductance. *Nat. Commun.* **11**, 3690 <https://doi.org/10.1038/s41467-020-17538-1>

61 Sheng, X., Watanabe, A., Li, A., Kim, E., Song, C., Murata, K. et al. (2019) Structural insight into light harvesting for photosystem II in green algae. *Nat. Plants* **5**, 1320–1330 <https://doi.org/10.1038/s41477-019-0543-4>

62 Malone, L.A., Qian, P., Mayneord, G.E., Hitchcock, A., Farmer, D.A., Thompson, R.F. et al. (2019) Cryo-EM structure of the spinach cytochrome b₆f complex at 3.6 Å resolution. *Nature* **575**, 535–539 <https://doi.org/10.1038/s41586-019-1746-6>